Imaging small numbers of (single?) Ba atoms in solid xenon for barium tagging in nEXO

T. Walton,[1] C. Chambers,[1] A. Craycraft,[1] W. Fairbank Jr.,[1, *] J.B. Albert,[2] D.J. Auty,[3] P.S. Barbeau,[4] V. Basque,[5] D. Beck,[6] M. Breidenbach,[7] T. Brunner,[8, 9] G.F. Cao,[10] B. Cleveland,[11, †] M. Coon,[6] T. Daniels,[7] S.J. Daugherty,[2] R. DeVoe,[8] T. Didberidze,[3] J. Dilling,[12] M.J. Dolinski,[13] M. Dunford,[5] L. Fabris,[14] J. Farine,[11] W. Feldmeier,[15] P. Fierlinger,[15] D. Fudenberg,[8] G. Giroux,[16, ‡] R. Gornea,[5, 16] K. Graham,[5] G. Gratta,[8] M. Heffner,[17] M. Hughes,[3] X.S. Jiang,[10] T.N. Johnson,[2] S. Johnston,[18] A. Karelin,[19] L.J. Kaufman,[2] R. Killick,[5] T. Koffas,[5] S. Kravitz,[8] R. Krücken,[12] A. Kuchenkov,[19] K.S. Kumar,[20] D.S. Leonard,[21] C. Licciardi,[5] Y.H. Lin,[13] J. Ling,[6] R. MacLellan,[22] M.G. Marino,[15] B. Mong,[11] D. Moore,[8] A. Odian,[7] I. Ostrovskiy,[8] A. Piepke,[3] A. Pocar,[18] F. Retiere,[12] P.C. Rowson,[7] M.P. Rozo,[5] A. Schubert,[8] D. Sinclair,[12, 5] E. Smith,[13] V. Stekhanov,[19] M. Tarka,[20] T. Tolba,[16] K. Twelker,[8, §] J.-L. Vuilleumier,[16] J. Walton,[6] M. Weber,[8] L.J. Wen,[10] U. Wichoski,[11] L. Yang,[6] Y.-R. Yen,[13] and Y.B. Zhao[10]

(nEXO Collaboration)

[1] *Physics Department, Colorado State University, Fort Collins CO, USA*
[2] *Physics Department and CEEM, Indiana University, Bloomington IN, USA*
[3] *Department of Physics and Astronomy, University of Alabama, Tuscaloosa AL, USA*
[4] *Department of Physics, Duke University, and Triangle Universities Nuclear Laboratory (TUNL), Durham North Carolina, USA*
[5] *Physics Department, Carleton University, Ottawa ON, Canada*
[6] *Physics Department, University of Illinois, Urbana-Champaign IL, USA*
[7] *SLAC National Accelerator Laboratory, Stanford CA, USA*
[8] *Physics Department, Stanford University, Stanford CA, USA*
[9] *Department of Physics, McGill University, Montreal QC, Canada*
[10] *Institute of High Energy Physics, Beijing, China*
[11] *Department of Physics, Laurentian University, Sudbury ON, Canada*
[12] *TRIUMF, Vancouver BC, Canada*
[13] *Department of Physics, Drexel University, Philadelphia PA, USA*
[14] *Oak Ridge National Laboratory, Oak Ridge TN, USA*
[15] *Technische Universitat Munchen, Physikdepartment and Excellence Cluster Universe, Garching, Germany*
[16] *LHEP, Albert Einstein Center, University of Bern, Bern, Switzerland*
[17] *Lawrence Livermore National Laboratory, Livermore CA, USA*
[18] *Amherst Center for Fundamental Interactions and Physics Department, University of Massachusetts, Amherst MA, USA*
[19] *Institute for Theoretical and Experimental Physics, Moscow, Russia*
[20] *Department of Physics and Astronomy, Stony Brook University, SUNY, Stony Brook NY,USA*
[21] *New place in S. Korea*
[22] *Department of Physics, University of South Dakota, Vermillion SD, USA*
(Dated: May 19, 2016)

Images of Ba atoms in solid Xe in a focused laser region, after deposition from vacuum onto a cold sapphire window, are obtained using a 619-nm fluorescence peak down to the single-atom level. This is an important step toward Ba tagging with a cryogenic probe from liquid Xe for the nEXO neutrinoless double beta decay experiment.

I. INTRODUCTION

The search for neutrinoless double beta decay ($0\nu\beta\beta$) is an important probe into the nature of neutrinos. Observation would require that neutrinos are Majorana particles, would demonstrate violation of lepton number conservation, and could help determine the absolute neutrino mass [1]. EXO-200 is searching for $0\nu\beta\beta$ in ^{136}Xe with around 170 kg

---
* Corresponding author
† Also SNOLAB, Sudbury ON, Canada
‡ Now at Queen's University, Kingston ON, Canada
§ Now at WiTricity, Watertown, MA

of liquid Xe (lXe) enriched to 80.6% ^{136}Xe in a dual time projection chamber (TPC). Two-neutrino double beta decay ($2\nu\beta\beta$) of ^{136}Xe has been observed by EXO-200, and its half-life is measured at $T_{1/2}^{2\nu\beta\beta} = 2.165 \pm 0.016(\text{stat}) \pm 0.059(\text{sys}) \times 10^{21}$ yr [2]. The most recent EXO-200 $0\nu\beta\beta$ search sets a limit on the half-life at $T_{1/2}^{0\nu\beta\beta} < 1.1 \times 10^{25}$ yr (90% CL), which corresponds to an effective Majorana neutrino mass of $\langle m_{\nu_e} \rangle$ <190-450 meV, depending on nuclear matrix element calculations [3].

A liquid ^{136}Xe TPC provides a unique opportunity to tag the daughter ^{136}Ba at the site of a double beta decay event. The implementation of this Ba tagging would improve $0\nu\beta\beta$ sensitivity by effectively eliminating all backgrounds except $2\nu\beta\beta$ [4]. Ba tagging is being investigated for possible incorporation in the next-generation ton-scale lXe experiment, nEXO. Initial results have been reported for research on methods of Ba tagging in lXe [5, 6], and also in a Xe gas TPC [7]. This paper presents additional progress towards realization of Ba tagging in solid Xe (sXe) for nEXO. In this method, a cryogenic probe would be moved to the position of the $0\nu\beta\beta$ candidate event, and the daughter atom or ion would be captured in a small amount of sXe at the end of the probe. It would then be detected by its laser-induced fluorescence in the sXe [5]. It is expected that a Ba^{++} ion will neutralize once to Ba$^+$ in lXe, as the lXe conduction band gap is slightly less than the ionization potential for Ba$^+$ [4]. Neutralization to Ba may also occur in the charge cloud following a $\beta\beta$ event. A new study of ^{214}Bi daughters of ^{214}Pb β-decay in EXO-200 has reported that 76(6)% of these daughters are ionized, with negligible subsequent neutralization after many minutes [8]. Thus, a high percentage of ^{136}Ba $0\nu\beta\beta$ daughters may be expected in the single ionized state in lXe. Whether or not the ^{136}Ba will remain ionized in sXe on a cold probe is not yet known.

Significant progress on understanding the spectroscopy of Ba in sXe has been made recently [5, 9]. An image of $\leq 10^4$ Ba atoms was obtained with the strong fluorescence peaks at 577 and 591 nm. However, bleaching of these fluorescence peaks with laser exposure causes rapid reduction of the emission rate at these wavelengths at high laser intensity, e.g., using a focused beam. Thus obtaining large numbers of photons from single Ba atoms is difficult without a method to overcome bleaching, e.g., with repumping lasers. Imaging was not attempted in [5] using the peak at 619 nm, though this peak has weaker bleaching by many orders of magnitude. This peak is promising for imaging of smaller numbers of atoms
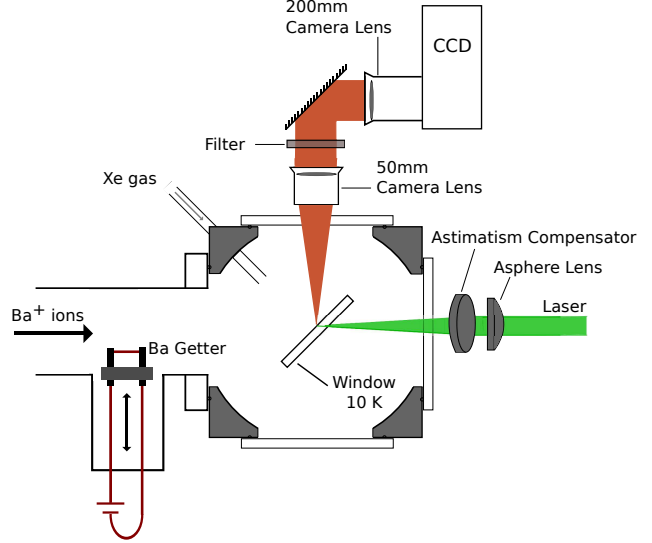

FIG. 1. Experimental setup for depositing Ba/Ba$^+$ in sXe matrices, and for excitation and imaging of the deposited atoms/ions.

because larger numbers of photons per atom may be obtained. This work focuses on imaging single Ba atoms in sXe via the low-bleaching 619-nm fluorescence. Varying numbers of atoms are observed in a focused laser region down to the single atom level.

II. APPARATUS AND METHOD

The apparatus for depositing and observing Ba/Ba$^+$ deposits in sXe is described in [5]. Important components are shown in Fig. 1. The source of Ba$^+$ is an ion beam at 2000 eV, filtered to select Ba$^+$ with an E×B velocity filter. A set of pulsing plates produces 1-μs pulses for depositing small numbers of ions. The spectra of Ba$^+$ ion deposits in the sXe matrix exhibit peaks known to be due to neutral Ba atoms [5]. Thus some percentage of the ions neutralize in the matrix, but the fraction has not yet been determined. An alternative source of neutral Ba is a BaAl$_4$ getter wire which can be moved into the beam path and heated to emit Ba atoms toward the sample. However, it is challenging to achieve low Ba flux with this source and to calibrate it.

Deposits are made on a cold sapphire window tilted at 45°. To create a sample, Xe gas is directed toward the window using a leak valve. The Xe gas freezes on the window and forms a sXe matrix with a thickness of around half a micron. This is initiated a few seconds prior to the Ba deposit, continues dur-

ing the Ba deposit, and is turned off a few seconds after the Ba deposit.

In this work, deposits are made with the sapphire window at around 50 K, partly to reduce hydrogen content in the matrix, as hydrogen condenses well below 50 K in vacuum [5]. The window is then cooled to 11 K for observation. Deposits made at 50 K result in higher 619-nm signal than those made at 11 K. Xe deposition at around 30 nm/s also results in higher 619-nm signal, as compared to lower leak rates, while not being so high as to result in a frosty Xe matrix. An experiment cycle consists of a deposit at 50 K, a fluorescence observation at 11 K, and then the deposit is evaporated by heating the window to 100 K. Many deposits are made in a day with varying numbers of ions deposited, as well as periodic Xe-only deposits to establish the background.

The excitation laser, a Coherent 599 cw dye laser with Rhodamine 6G dye pumped by the 514-nm line of a Lexel 3500 argon ion laser, enters from the back side of the window. Ba fluorescence light is collected and collimated by a 50 mm Nikon camera lens. A band-pass filter with FWHM of 20 nm passes just the 619-nm fluorescence peak. A 200 mm Nikon camera lens then focuses the image onto a liquid nitrogen cooled CCD, resulting in an image of $4\times$ magnification. Each of the 20×20 μm pixels of the CCD represents approximately a 5×5 μm area on the sXe sample.

For a given laser intensity, the smallest focus possible is desired for optimal signal-to-noise from single atoms. To achieve this, an aspherical lens of 7.9 cm focal length [10] is used to minimize spherical aberration, and a fused silica optical flat of 1 cm thickness is placed at 10° after the lens in order to compensate for astigmatism caused by the tilted sapphire window (Fig. 1).

Vibrations of the sapphire relative to the excitation laser must also be considered, as this will increase the area of laser exposure, and thus the number a Ba atoms illuminated. Though the number of Ba atoms instantaneously exposed is independent of vibrations, reducing the effectively exposed area is desirable in clarifying the definition of the laser region. To reduce the exposed region, a shutter, placed the laser path, is synchronized with the signal from an accelerometer on the outside of the cryostat, such that the laser exposure is reduced to one lobe of the sinusoidal vibration. Measurements of these vibrations and the effect of the synchronized shutter are discussed in Section III C.
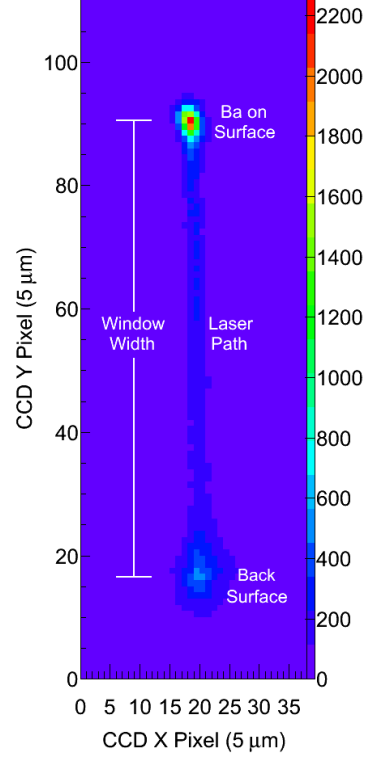

FIG. 2. Example image of a Ba^+ deposit in sXe on a tilted c-plane sapphire window of 0.5 mm thickness.

III. RESULTS

A typical image made with a focused laser beam at 570 nm is shown in Fig. 2. Weak fluorescence of impurities (most likely ppb of Cr^{3+}) in the sapphire window is seen along the laser's path as a weak vertical line. At both ends, some background emission from the surfaces is observed. At the front surface (at the top in the image), extra fluorescence is detected from a small number of Ba atoms within the focused laser.

The number of Ba^+ ions deposited within the $1/e$ radius of the laser beam gives a rough upper limit to the number of Ba atoms responsible for the observed signal. For typical ion pulses of 13 fC/pulse and focused laser $1/e^2$ radii of $w_{0x} = 2.06$ μm and $w_{0y} = 2.66$ μm, this results in about 0.035 Ba^+ ions/pulse in the $1/e$ intensity laser region. The signal in Fig. 2 corresponds to a deposit of about 10 Ba^+ ions into the laser region, and is therefore roughly due to ≤ 10 Ba atoms. Deposits of ≤ 39, ≤ 3, and ≤ 1 Ba atoms are shown in Fig. 3a,b,c, respectively, with Xe-only deposits made before and after each Ba^+ deposit.
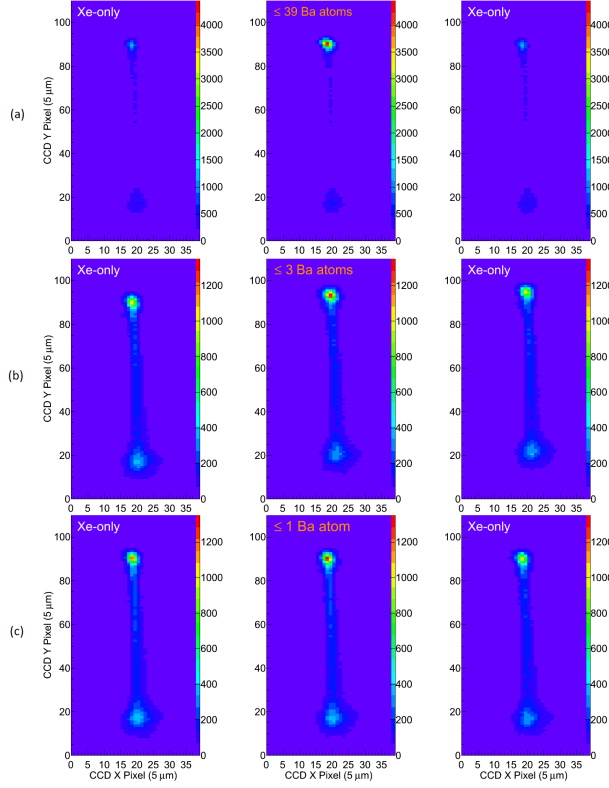
FIG. 3. Images of Ba$^+$ deposits yielding (a) ≤ 39, (b) ≤ 3, and (c) ≤ 1 Ba atoms in the focused laser region, with Xe-only deposits done before and after each respective Ba$^+$ deposit. Exposures are 60 s with around 0.15 mW of 570-nm laser excitation. Needs new.
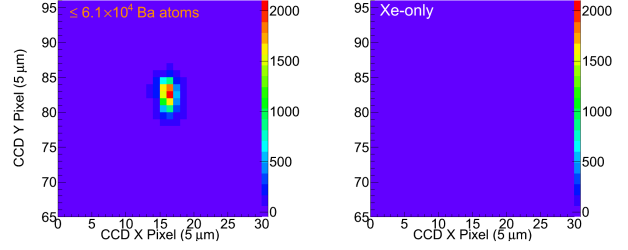

FIG. 4. Image of a Ba$^+$ deposit yielding $\leq 6.1 \times 10^4$ Ba atoms with its succeeding Xe-only deposit. Exposures are 0.5 s with around 1.1 mW of 572-nm laser excitation. Needs new.
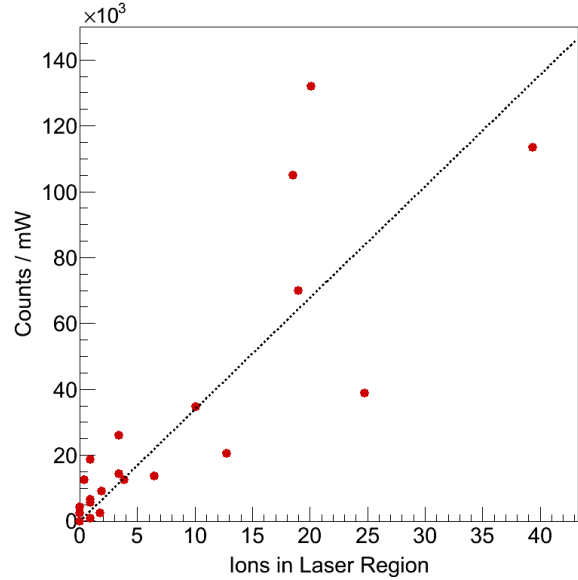

FIG. 5. 619-nm Ba fluorescence vs. number of ions deposited. Exposures are around ? s with around ? mW of 572-nm laser excitation. Old: Exposures are 60 s with around 0.15 mW of 570-nm laser excitation.

The background level is determined by averaging the summed CCD counts in the focused laser region from the two surrounding Xe-only deposits for each Ba$^+$ deposit. The Ba fluorescence counts are determined by subtracting this background from the total counts in the same laser beam region in the image of the Ba$^+$ deposit. A significant finding is that after a large deposit of $\leq 6.1 \times 10^4$ Ba atoms, the background in the next Xe-only deposit is the same as the Xe-only run before this deposit, as shown in Fig. 4.*[We need one with an actual preceding Xe run, and need to look on lower scale at any BG change. Also, may want not quite so large a deposit – we actually don't know yet how large deposits affect it]* This is important for the implementation of this Ba tagging method in nEXO, i.e., false positives will not occur from previous Ba tags.

The Ba counts vs. Ba$^+$ ions deposited in the laser region are plotted in Fig. 5. The summed CCD counts in the laser region in sXe of each image is

linear with ions deposited. The observed signal corresponds to 3400 ± 360 counts/mW per atom with around 0.15 mW of focused 572-nm laser excitation, around ? s of laser exposure. Exact exposure times vary slightly according to the total open time of the vibration compensation shutter, as discussed in Section III C. Counts are scaled by the integral of the power signal recorded by a power meter after the laser shutter. Background-subtracted images of deposits near the linear trend line are shown in Fig. 6 corresponding to (a) ≤ 10 atoms, (a) ≤ 3 atoms, and (a) ≤ 1 atom. These represent the expected signal level, with a clear peak at the single-atom level.

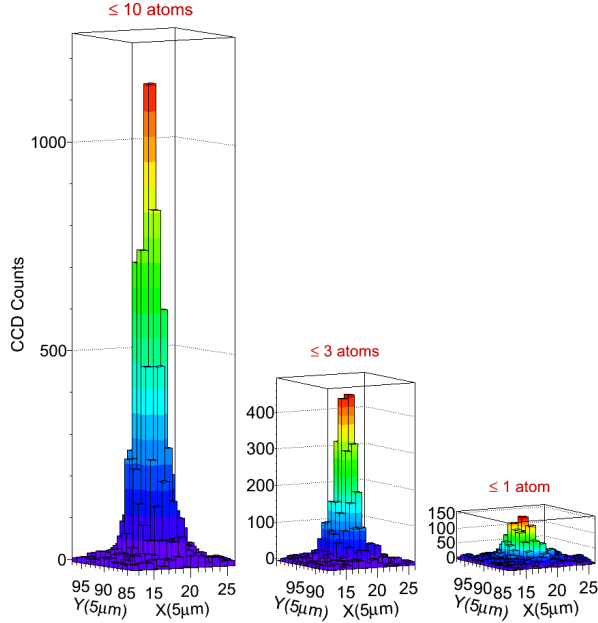**Old paragraph, for the 8-7 plot:** The Ba

FIG. 6. Subtracted images of 619-nm fluorescence in the focused laser region for runs near the linear trend line in signal vs. ions deposited. Exposures are 60 s with around 0.15 mW of 570-nm laser excitation. Needs new.

counts vs. Ba^+ ions deposited in the laser region are plotted in Fig. 5. The summed CCD counts in the laser region in sXe of each image is linear with ions deposited, albeit with significant scatter due to ion beam instabilities in this run. The observed signal corresponds to 3400 ± 360 counts/mW per atom with around 0.15 mW of focused 570-nm laser excitation, and 60-s CCD exposures. Counts are scaled by laser power to account for small variations in laser power. Background-subtracted images of deposits near the linear trend line are shown in Fig. 6 corresponding to (a) ≤ 10 atoms, (a) ≤ 3 atoms, and (a) ≤ 1 atom. These represent the expected signal level, with a clear peak at the single-atom level.

A Gaussian fit to the images gives a $1/e^2$ radius of 12 μm, which is much larger than the average laser beam radius of w = 2.4 μm. Aberrations and vibrations in the collection optics and imperfections in the surface of the sXe layer could contribute to blurring of the image.
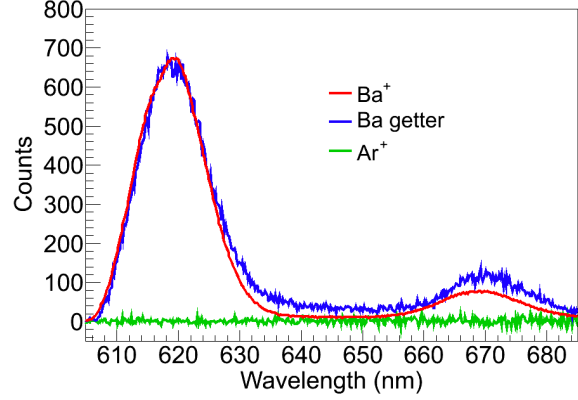

FIG. 7. Observation of deposits from three different sources in sXe. Curves are scaled due to different deposit sizes.

A. Identification of 619-nm Peak as Ba in sXe

Spectra of neutral Ba deposits made with the Ba getter source are compared to spectra of a Ba^+ deposit in Fig. 7. Identical spectra are observed using the different sources under similar deposit conditions. This confirms that the images measured are of Ba atoms resulting from neutralization of the incident Ba^+ ions. Another peak at 670 nm which is mentioned in [5] is also attributed to Ba. No similar fluorescence is observed from deposits of Ar^+ ions in sXe (Fig. 7) at 2000 eV under the same conditions. This rules out matrix damage, e.g. fluorescent color centers, as the source of the 619-nm peak. The linearity of the fluorescence signal vs. number og Ba^+ ions at low flux supports an assignment to atomic Ba, as opposed to molecular Ba_2

B. Backgrounds

Very low concentrations of Cr^{3+} in the sapphire bulk (sub-ppb level) produce a strong fluorescence at 693 nm, with a broad tail extending to the 610-630 nm region passed by the band-pass filter. This produces the faintly visible line through the sapphire window discussed above. The broad fluorescence is also assigned to Cr^{3+}, as its excitation spectrum is identical to that of the well-known lines around 693 nm. Commercially available c-plane quality sapphire from Meller Optics and Rubicon Technologies has sufficiently low concentrations for detecting single Ba atoms.

The background emission from the sapphire sur-

5

face is the main challenge for single Ba imaging. It has been found that this background can be reduced significantly and semi-permanently by bleaching. A variety of wavelengths have been used for bleaching, including 514.5 nm, 532 nm, 570-572 nm, and 580.5 nm. The set of deposits used for Fig. 5 was done after an overnight raster scan of a 20 mW 532 nm laser, focused to around $w_0 = 10$ μm, in a ?$\times$? position grid, with ? μm grid spacing and ? s at each position, in a repeating scan. This amounted to about ? minutes of exposure at each location, effectively eliminating the surface background over a region of about ?$\times$? μm, which is large enough to accommodate typical drift of the laser beam throughout a day. This was done with the sapphire window at 105 K.

C. Vibration Compensation

Vibrations of the sapphire window relative to the excitation laser were studied by observing movement of a "dust spot" on the sapphire window relative to the image of the laser on time scales down to 50 ms. Dust spots are highly scattering objects which are fixed to the sapphire window. They can be avoided when imaging Ba deposits, however they are useful in studies like this. The relative position of a dust spot and the laser, determined with 2D Gaussian fits to the raw images, are plotted in Fig. 8a, with a sampling of 200 50-ms frames, each separated by ? s of readout time. 2D Gaussian functions of width $w_x = 2.06$ μm and $w_y = 2.66$ μm, representing the minimum laser spot size, are overlain on each of these points and summed in Fig. 8b, thus representing the total laser exposure on the sapphire window. Sinusoidal vibration results in the majority of exposure occurring in two lobes.

As described in Section II, a shutter on the laser path was synchronized with the signal from an accelerometer on the cryostat, in order to isolate the exposure to one vibration lobe. A typical vibration signal is shown in Fig. 9. The 2.5 Hz frequency of the large spikes in the vibration signal is consistent with the audible frequency of the cryostat's He pump. The shutter is triggered by the large spikes, with a specified delay time and open time. It was determined that about 40 ms of delay time and 200 ms open time are optimal, resulting in laser exposure on only one of the vibration lobes, as shown in Fig. 8c.
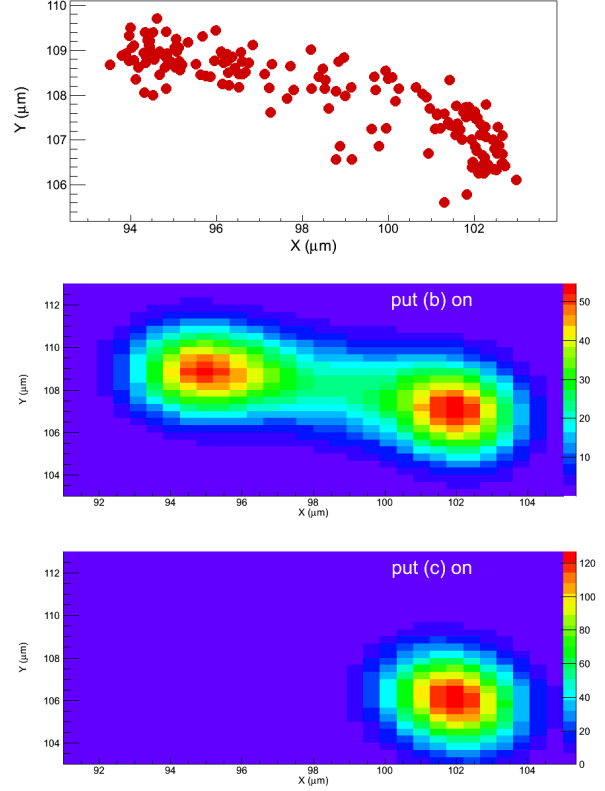

FIG. 8. Placeholder *[Plotting these on the same range like this makes it more clear.] Explain in caption how (b) and (c) are 1-amplitude gaus sums of [x] points or whatever they actually are...**and magnitudes are different, I guess there are more points in c?** Get axis labels/titles same size.*
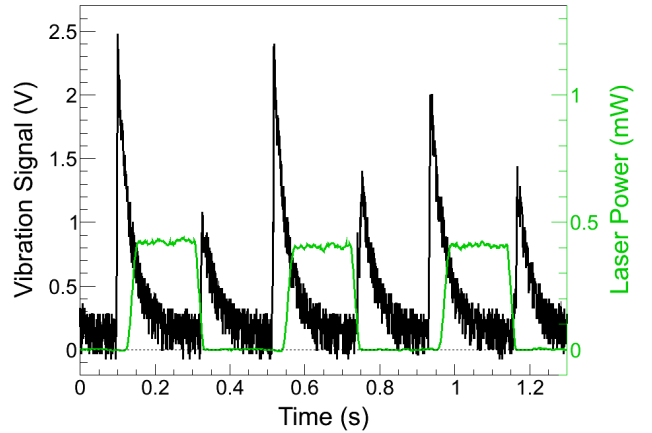

FIG. 9.

6

IV. CONCLUSIONS

The 619-nm emission peak observed in deposits of Ba^+ and Ba in sXe is attributed to neutral Ba in a stable and relatively abundant matrix site. Images of 619-nm fluorescence in a focused laser region from Ba atoms are achieved down to the single-atom level. Successful detection of Ba atoms in sXe at this level is a significant step toward Ba tagging in nEXO.

[1] K.A. Olive *et al.* (Particle Data Group), *Chin. Phys. C* **38**, 090001 (2014) (http://pdg.lbl.gov).

[2] J. Albert *et al.* (EXO-200 Collaboration), *Phys. Rev. C* **89**, 015502 (2014).

[3] J. Albert *et al.* (EXO-200 Collaboration), *Nature* **510**, 229 (2014).

[4] M. Moe, *Phys. Rev. C* **44**, R931 (1991).

[5] B. Mong *et al.*, *Phys. Rev. A* **91**, 022505 (1954).

[6] K. Twelker *et al.*, *Review of Scientific Instruments* **85**, 095114 (2014).

[7] T. Brunner *et al.*, *International Journal of Mass Spectrometry* **379**, 110-120 (2015).

[8] J. Albert *et al.* (EXO-200 Collaboration), *Phys. Rev. C* **92**, 045504 (2015).

[9] B. Davis, J. McCaffrey, *J. Chem. Phys.* **144**, 044308 (2016); doi: 10.1063/1.4940688

[10] Thorlabs part ASL10142-A.